OPTICAL REVIEW Vol. 21, No. 5 (2014) 541–544

Recording Characteristics of High-Density Thin Optical Disk Using Near-Field Optical Recording

Daiichi Koide*, Takeshi Kajiyama, Ryuji Sato, Haruki Tokumaru, and Yoshimichi Takano

Science and Technology Research Laboratories, NHK (Japan Broadcasting Corporation), Setagaya, Tokyo 157-8510, Japan

(Received January 9, 2014; Accepted March 31, 2014)

We report on the recording characteristics of a near-field optical recording thin optical disk (NFR-TOD). We proposed a new cooling-less-type write strategy for recording, applied it to the NFR-TOD experimental system, and also applied a partial response maximum likelihood (PRML) signal processing, which was evaluated and optimized the PR coefficient for playback signals of the prototype NFR-TOD. The NFR-TOD has a track pitch of 160 nm and improved recording characteristics. The experimental results of the prototype NFR-TOD and the system indicate sufficiently low bit error rates (bERs) for recorded data at a fourfold higher recording density than the current Blu-ray disk.

Keywords: near-field optical recording, thin optical disk, solid immersion lens, high density, partial response maximum likelihood

1. Introduction

A near-field optical recording-thin optical disk (NFR-TOD) system using a solid immersion lens (SIL)[1] exhibits fourfold higher recording density than the current Blu-ray disc system.[2–16] It can exhibit a large capacity and a high-data transfer rate towards recording next-generation ultra-high-definition television [i.e., Super Hi-Vision (SHV), 7320 × 4320 pixels] video signals[17,18] for home-use. Fourfold higher density recording using NFR optical disks with 1.2-mm-thick disks has been reported,[12,14] and studies of larger capacity using multilayer recording using NFR have been reported.[15,16] If the NFR media can realize 250-Mbps-class high-speed recording and two- or three-layer recording, the SHV optical media, which has more than two hours recording ability would be able to be realized. Studies[19–23] on the maximum of sixteen-multilayer recording using far-field optical recording of the Blu-ray format have led to a data capacity of 2 TBytes the NFR system has a feasibility of the data capacity of 2 TBytes. Thin optical disks that have a thickness of about 0.1 mm can rotate at high speed,[24–26] and have demonstrated high-data transfer rate recording.[27–29] Although the NFR optical disk has a fourfold higher data capacity per recording layer than that of Blu-ray disk, the 20 nm gap servo control between the SIL optical head and the disk surface meant that there were difficulties with obtaining a high disk rotational speed for high-data transfer rate recording when the conventional method was used.[30–34] We have proposed a precise gap servo system of reducing harmonics of an axial run-out disturbance-feed-forward control (RHD-FFC) system for the NFR drive.[35] We have also proposed a high-density thin optical disk with a narrow track pitch for NFR with an SIL, and also have reported and indicated the feasibility of high-data transfer rate recording corresponding to 252 Mbps and indicated less than 2 nm of high-precision gap servo control with a small axial run-out between 1 and $10\,\mu\mathrm{m}_{\mathrm{p\text{-}p}}$, and obtained sufficient carrier-to-noise ratio characteristics at a high disk rotational speed.[36]

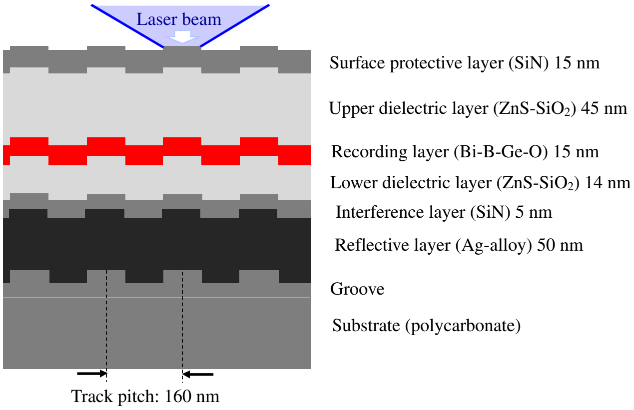

Fig. 1. (Color online) Configuration of NFR-TOD.

We report on the recording characteristics of an NFR-TOD by applying a partial response maximum likelihood (PRML) signal processing for reproducing playback signals, and applying a new cooling-less-type write strategy (WS) for the NFR-TOD system. We evaluated the bit error rates (bERs) of recorded data on high-density thin optical disks.

2. Near-Field Optical Recording on High-Density Thin Optical Disk

2.1 High-density thin optical disk media

The configuration of a prototype NFR-TOD is shown in Fig. 1. The disk has recording tracks with a track pitch of 160 nm and a groove depth of 30 nm. The groove tracks were copied from a metal stamper, which was made by the heat-mode mastering method. The NFR-TOD consists of a stack of reflective, interference, lower dielectric, recording, upper dielectric, and surface protective layers on a thin substrate. The elements and thickness of each component are listed on the right. The recording layer is applied to an inorganic metal–oxide material of Bi–B–Ge–O, which has been used

---

*E-mail address: koide.d-jy@nhk.or.jp

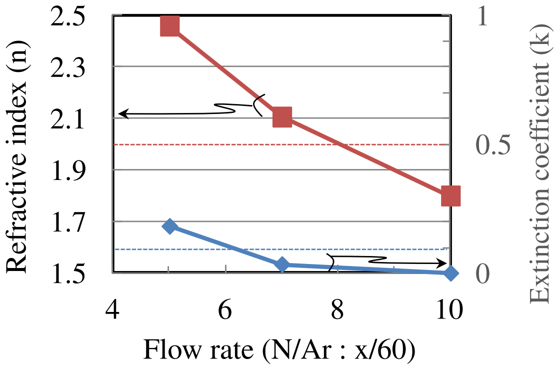

Fig. 2. (Color online) Characteristics of refractive index (*n*) and extinction coefficient (*k*) versus flow rate of N/Ar gases for forming SiN surface layer.

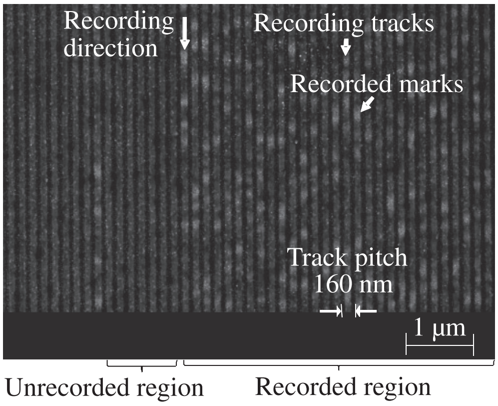

Fig. 3. Image of recording marks on a prototype NFR-TOD. The image was observed by scanning electron microscopy (SEM).

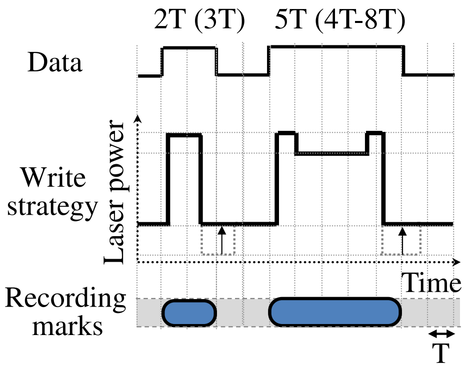

Fig. 4. (Color online) Cooling-less-type of write strategy (cl-WS) for NFR-TOD.

on a write-once-type thin optical disk.[28] These layers were made by using RF magnetron sputtering equipment. The surface protective layer was applied silicon nitride (SiN). The SiN surface layer was made by using an optimized nitrogen gas and Ar-sputtering gas ratio. Figure 2 shows the characteristics of refractive index (*n*) and extinction coefficient (*k*) versus flow rate of N/Ar gases for forming the SiN surface layer. The horizontal axis (*x*) shows the flow rate of N. When the N/Ar ratio of 7/60 was applied, the *n* obtained had a high reflective index (*n*) of 2.1 with suppressing to low *k*.

The recording experimental results were as follows: the jitter value was 17.8% when the conventional N/Ar gases flow rate of 10/60 was applied. When the optimized N/Ar gas flow rate of 7/60 was applied, the jitter value reduced to 15.0%.

Figure 3 shows an image of recording marks on the prototype NFR-TOD. This image was observed on the recording layer of the NFR-TOD by scanning electron microscopy (SEM). The recording marks that recorded random patterns of various lengths are shown on the right.

2.2 *Write strategy*

We propose a cooling-less-type-write strategy (cl-WS) for a write-once-type NFR-TOD. Figure 4 shows the shape of the cl-WS for the NFR-TOD. The WS was based on a castle-type WS and was improved for NFR. The recording power on near-field recording media was less than that of conventional far-field recording media. Thus, the effect of thermal accumulation and diffusion in the recording layer on the NFR media could be ignored. As the cooling process was omitted and simply drove the laser emission, the timing of laser emission could be precisely controlled.

As the recording experimental results, the jitter value was 15.0% when the conventional castle-type WS was applied. When the cl-WS was applied, the jitter value could reduce to 14.4%.

2.3 *Applying partial response maximum likelihood (PRML) on NFR-TOD*

This time, the PRML signal processing was applied for playback signal[37] for NFR-TOD. To evaluate and obtain a low bit error rate, we have made a prototype PRML signal processing system for the NFR-TOD system (on Fig. 5). The PRML signal processing system was composed of the large scale integrated (LSI) circuits and it was embedded with some PR coefficients to be able to process in real time for the playback data. Because the calculation was simple and the processing was fast, we prepared the PR coefficients of PR(121), PR(1331), and PR(1221).[38] Applying the signal processing system, we investigated the recording and playback and measured the bit error rates of the NFR-TOD.

3. Experimental Procedure

3.1 *Experimental conditions*

Figure 5 shows the configuration of the NFR-TOD experimental setup. An SIL was used on the optical head based on the NFR optical disk drive system. The mechanical stabilizer was close to the rotational disk. Table 1 summarizes the specifications for the experimental set-up. The optical head was applied LAH79 SIL. The gap distance between the SIL optical head surface and the disk surface was adjusted to 20 nm, and the gap servo and tracking servo were operated. The PRML signal processing system was prepared and applied for playback signals. We recorded the random pattern data and evaluated the playback signal by applying some PR equalizations and Viterbi detection.

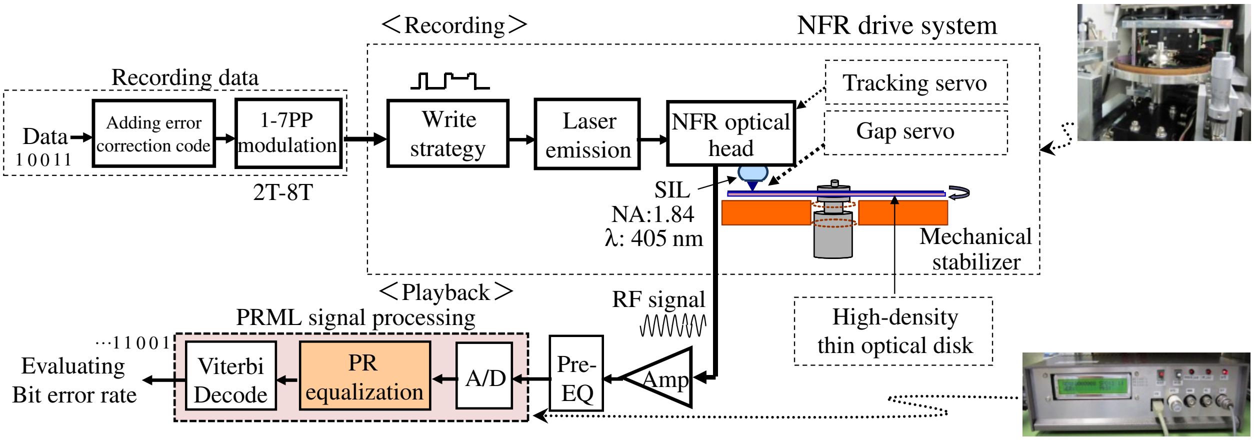

Fig. 5. (Color online) Configuration of experimental setup. The system included the prototype PRML processing system.

Table 1. Specifications of experimental setup.

Laser wavelength (nm)	405
NA (objective lens)	1.84
Track pitch of disk (nm)	160
Disk capacity (GBytes)	100
Gap length (nm)	20
Recording modulation	1–7PP
Detection method of palyback signal	PR + Viterbi

Table 2. Conditions of recording laser powers.

Top write power (mW)	3.45
Middle write power (mW)	3.40
Bias power (mW)	1.15
Conventional cooling power (mW)	0.05
Read power (mW)	0.21

Table 3. Characteristics of PRSNR.

PR coefficients	PR(121)	PR(1331)	PR(1221)
PRSNR	8.1	11.2	14.1

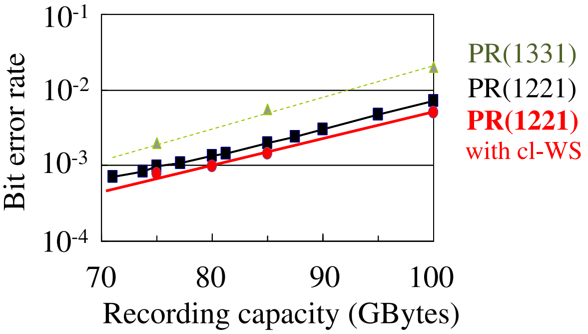

Fig. 6. (Color online) Bit-error-rate characteristics of NFR-TOD.

3.2 *Experimental results*

We evaluated the recording characteristics of NFR-TOD. Table 2 summarizes the conditions of recording laser powers when the data transfer rate was 36 Mbps. First, we evaluated the signal-to-noise ratio when various PR-equalization coefficients were applied at the same speed. Table 3 shows PRSNR[39)] characteristics versus PR coefficients. When the PR coefficient of PR(1221) was applied, PRSNR obtained the highest value of 14.1, which was above those of PR(1331) and PR(121).

We then evaluated the bit-error-rate (bER) characteristics when the recording capacity with linear density was varied. Figure 6 plots the bER characteristics vs the recording capacity for the NFR-TOD. The bER characteristics increased with recording capacity. When PR(1331) was applied, many bit errors were detected. When PR(1221) was applied, the bER was reduced compared with that when PR(1331) was applied. When the improved WS was applied, the bER was further suppressed. The bER of 1×10^{-3} was obtained at a rate corresponding to 80 GBytes, and the bER of 5×10^{-3} was obtained corresponding to 100 GBytes. We think that the media would obtain lower bER for higher reliability when the material composition ratio of a recording layer of the media is strictly optimized.

We found that the prototype NFR-TOD and the system would have capable performances for recording and playing video data when not only an error correcting code (ECC) of the current Reed-Solomon code but also a robust ECC of low-density parity-check code was applied.

4. Conclusions

We confirmed that the prototype NFR-TOD had sufficient recording characteristics on the NFR experimental system by improving the recording media, applying a new write strategy, and applying the optimized PRML signal processing for the playback signal. The NFR-TOD system and the experimental results indicate the possibility of high-density recording and playback of high-quality video data.

Acknowledgement

The authors greatly thank Memory-Tech Corporation for cooperating to provide a disk stamper and thank everyone who cooperated on this work.

References

1) S. M. Mansfield, W. R. Studenmund, G. S. Kino, and K. Osato: Opt. Lett. **18** (1993) 305.
2) I. Ichimura, K. Kishima, K. Saito, K. Yamamoto, Y. Kuroda, A. Iida, S. Masuhara, and K. Osato: Jpn. J. Appl. Phys. **40** (2001) 1821.
3) M. Shinoda, K. Saito, T. Kondo, T. Ishimoto, and A. Nakaoki: Jpn. J. Appl. Phys. **42** (2003) 1101.
4) M. Shinoda, K. Saito, T. Ishimoto, T. Kondo, A. Nakaoki, N. Ide, M. Furuki, M. Takeda, Y. Akiyama, T. Shimouma, and M. Yamamoto: Jpn. J. Appl. Phys. **44** (2005) 3537.
5) M. Shinoda, K. Saito, T. Ishimoto, T. Ito, A. Nakaoki, M. Yamamoto, O. Maeda, T. Hashizu, T. Asano, K. Aga, K. Takagi, and M. Tazoe: Jpn. J. Appl. Phys. **45** (2006) 1321.
6) M. Shinoda, K. Saito, T. Kondo, A. Nakaoki, M. Furuki, M. Takeda, M. Yamamoto, T. J. Schaich, B. M. van Oerle, H. P. Godfried, P. A. C. Kriele, E. P. Houwman, W. H. M. Nelissen, G. J. Pels, and P. G. M. Spaaij: Jpn. J. Appl. Phys. **45** (2006) 1311.
7) M. Shinoda, K. Saito, T. Kondo, M. Furuki, M. Takeda, A. Nakaoki, M. Sasaura, and K. Fujiura: Jpn. J. Appl. Phys. **45** (2006) 1332.
8) C. A. Verschuren, D. M. Bruls, B. Yin, J. M. A. van den Eerenbeemd, and F. Zijp: Jpn. J. Appl. Phys. **46** (2007) 3889.
9) T. Ishimoto, S. Kim, T. Yamasaki, T. Yukumoto, A. Nakaoki, and M. Yamamoto: Jpn. J. Appl. Phys. **46** (2007) 3981.
10) T. Ishimoto, S. Kim, A. Nakaoki, T. Kondo, T. Mizukuki, and O. Kawakubo: Jpn. J. Appl. Phys. **47** (2008) 5814.
11) T. Ishimoto, A. Nakaoki, K. Saito, T. Yamasaki, T. Yukumoto, S. Kim, T. Kondo, T. Mizukuki, O. Kawakubo, M. Honda, N. Shinohara, and N. Saito: Jpn. J. Appl. Phys. **48** (2009) 03A015.
12) A. Nakaoki, O. Kawakubo, T. Ohkubo, T. Watanabe, and T. Yamagami: Jpn. J. Appl. Phys. **48** (2009) 03A042.
13) N. Yamaoka, T. Tagiri, Y. Higashika, K. Ishiguro, S. Ohshima, M. Yamaguchi, T. Takishita, and F. Yokogawa: Jpn. J. Appl. Phys. **47** (2008) 5955.
14) K. Kitano, A. Yamaguchi, M. Miura, K. Horikawa, T. Tagiri, E. Muramatsu, S. Taniguchi, and F. Yokogawa: Tech. Dig. Int. Symp. Optical Memory and Optical Data Storage, 2008, TD05-167.
15) M. Birukawa, E. Ito, K. Narumi, R. Kojima, N. Yamada, T. Mizukuki, A. Nakaoki, and O. Kawakubo: Tech. Dig. Int. Symp. Optical Memory and Optical Data Storage, 2008, TD05-152.
16) K. Narumi, K. Hisada, T. Mihara, H. Habuta, K. Hayashi, Y. Tanaka, K. Sano, H. Tomita, T. Shiono, S. Furumiya, R. Kojima, M. Birukawa, and N. Yamada: Jpn. J. Appl. Phys. **50** (2011) 09MG01.
17) M. Sugawara, M. Kanazawa, K. Mitani, H. Shimamoto, T. Yamashita, and F. Okano: SMPTE Motion Image J. **112** (2007) 377.
18) Y. Shishikui, K. Iguchi, S. Sakaida, K. Kazui, and A. Nakagawa: Proc. IEEE **101** (2013) 130.
19) I. Ichimura, K. Saito, T. Yamasaki, and K. Osato: Appl. Opt. **45** (2006) 1794.
20) A. Mitsumori, T. Higuchi, T. Yanagisawa, M. Ogasawara, S. Tanaka, and T. Iida: Jpn. J. Appl. Phys. **48** (2009) 03A055.
21) T. Nishihara, A. Tsuchino, Y. Tomekawa, H. Kusada, R. Kojima, and N. Yamada: Jpn. J. Appl. Phys. **50** (2011) 062503.
22) T. Kikukawa, M. Inoue, A. Kosuda, and T. Ushida: Jpn. J. Appl. Phys. **50** (2011) 09MF02.
23) M. Ogasawara, K. Takahashi, M. Nakano, M. Inoue, A. Kosuda, and T. Kikukawa: Jpn. J. Appl. Phys. **50** (2011) 09MF01.
24) Y. Aman, N. Onagi, S. Murata, Y. Sugimoto, D. Koide, and H. Tokumaru: Jpn. J. Appl. Phys. **46** (2007) 3750.
25) T. Kajiyama, D. Koide, H. Tokumaru, Y. Takano, N. Onagi, and Y. Aman: Jpn. J. Appl. Phys. **50** (2011) 09MC07.
26) H. Hwang, J.-G. Kim, K. W. Song, K.-S. Park, N.-C. Park, H. Yang, Y.-C. Rhim, and Y.-P. Park: Jpn. J. Appl. Phys. **50** (2011) 09MC04.
27) D. Koide, Y. Takano, H. Tokumaru, N. Onagi, Y. Aman, S. Murata, Y. Sugimoto, and K. Ohishi: Jpn. J. Appl. Phys. **47** (2008) 5822.
28) D. Koide, Y. Takano, H. Tokumaru, N. Onagi, Y. Aman, S. Murata, Y. Sugimoto, and K. Ohishi: IEEE Trans. Magn. **45** (2009) 2190.
29) D. Koide, T. Kajiyama, H. Tokumaru, Y. Takano, N. Onagi, Y. Aman, and K. Ohishi: Jpn. J. Appl. Phys. **49** (2010) 08KC04.
30) K. Saito, T. Ishimoto, T. Kondo, A. Nakaoki, S. Masuhara, M. Furuki, and M. Yamamoto: Jpn. J. Appl. Phys. **41** (2002) 1898.
31) T. Ishimoto, K. Saito, M. Shinoda, T. Kondo, A. Nakaoki, and M. Yamamoto: Jpn. J. Appl. Phys. **42** (2003) 2719.
32) T. Ishimoto, T. Matsui, S. Kim, K. Saito, K. Takagi, S. Haga, A. Nakaoki, and M. Yamamoto: Proc. SPIE **6282** (2006) 62820C.
33) D. M. Bruls, J. I. Lee, C. A. Verschuren, J. M. A. van den Eerenbeemd, F. Zijp, and B. Yin: Proc. SPIE **6282** (2006) 62820F.
34) J.-K. Seo, J. U. Lee, Y. S. Shin, J.-M. Park, I. H. Choi, and B.-H. Min: Proc. SPIE **6282** (2006) 62820E.
35) D. Koide, T. Kajiyama, H. Tokumaru, Y. Takano, Y. Nabata, T. Ogata, T. Miyazaki, and K. Ohishi: Jpn. J. Appl. Phys. **51** (2012) 08JA04.
36) D. Koide, T. Kajiyama, R. Sato, H. Tokumaru, Y. Takano, and K. Ohishi: Jpn. J. Appl. Phys. **52** (2013) 09LG01.
37) T. Iwanaga, S. Ohkubo, M. Nakano, M. Kubota, H. Honma, T. Ide, and R. Katayama: Jpn. J. Appl. Phys. **42** (2003) 1042.
38) M. Kobayashi and T. Iwanaga: in *PRML Signal Processing Technologies*, ed. K. Arai (Triceps, 1996) Chaps. 7, 8 [in Japanese].
39) M. Ogawa, M. Nakano, S. Ohkubo, H. Honma, T. Ichimura, and T. Iwanaga: Jpn. J. Appl. Phys. **43** (2004) 4863.